Synthesis and Characterization of Glucose-Bis(pyrazole)–Cu(II)/Ni(II) Complexes and Their *in Vitro* DNA Binding Studies

Sartaj TABASSUM* and Irshad-ul-Haq BHAT

Department of Chemistry, Aligarh Muslim University; Aligarh–202002, India.
Received September 5, 2009; accepted December 11, 2009; published online December 21, 2009

The D-glucose-bis pyrazolyl complexes of Cu(II) 1 and Ni(II) 2 were synthesized and characterized by elemental analysis, molar conductance measurements and spectroscopic methods. The solution structures of the complex have been assessed to square pyramidal using electronic absorption and electronic paramagnetic resonance (EPR) spectroscopy. The interaction of 1 and 2 with calf thymus DNA (CT DNA) has been carried out by absorption, emission, viscometric and electrochemical methods. The intrinsic binding constant K_b was determined as $13.4\times10^5\,M^{-1}$, $4.5\times10^5\,M^{-1}$ for 1 and 2, respectively suggestive of strong binding of complexes with DNA. Furthermore, higher value of K_b for 1 implies that this complex interacts more strongly with CT DNA in comparison to 2. The quenching constant "*K*" of 1 and 2 obtained from emission spectral methods was 1.33, 0.55, respectively. Complex 1 hydrolytically cleaved pBR322 supercoiled DNA in absence of an activating agent. The enhanced cleavage of pBR322 DNA was observed in presence of ascorbic acid as a reducing agent, 1 also displays efficient photonuclease activity through double strand DNA breaks when irradiated at 365 nm through mechanistic pathway involving hydroxyl radicals. In addition to the above binding studies, an *in vitro* binding study of complex 1 with protein human serum albumin (HSA), tyrptophan and mixtures of HSA, L-tryptophan with CT DNA was carried out. The *in vitro* "binding study" also supports that 1 shows higher binding affinity towards CT DNA.

Key words glucose-bis pyrazole; metal complex; *in vitro* binding study; human serum albumin; pBR322 DNA cleavage

In the forefront is the recent area of glycobiology a "sweet and safe" approach for the development of new drugs in medicinal inorganic chemistry.[1] The use of glycosyl substituents for enhanced tissue target, improved solubility and reduced toxicity has attracted many researchers to explore the possibility of carbohydrate-based drug strategies.[2—5] Chen *et al.* have synthesized a novel carbohydrate linked to cisplatin analogue, *cis*-dichloro[(2-β-D-glucopyranosidyl)-propane-1,3-diamine]platinum and examined selective cytotoxicity towards cancer cells.[6] This complex exhibits specific *in vitro* antitumour activity against human ovarian cancer cell A2780S and human melanoma cancer cell MeWo. Some of the cancer cell antigens are carbohydrates and several trials are being carried out to develop carbohydrate derived cancer vaccines.[7] Globo H is a prominent epitope on cancer cells; therefore a potential vaccine was prepared consisting of the synthetic hexasaccharide chain of Globo H linked to KLH.[8]

Recently, Nakase *et al.* have demonstrated artemisinin tagged to transferrin *via* carbohydrate chain exhibits high potency and specificity against cancer cells.[9] Carbohydrate linked to biologically relevant molecules like pyrazole and imidazole act as an attractive scaffold for transition metal ions.[10—12] The interaction of transition metal–saccharide complexes with DNA is significantly important (DNA is one of the main molecular targets in the action of anticancer drugs), as many naturally occurring antitumour agents are capable of modifying nucleic acids only in presence of metal ions and oxygen.[13—16] Of these antitumour agents, a vast majority usually contains sugar derivatives as their back bone. Thus, there has been profound interest in the design, study of DNA binding and cleavage properties of glucose-derived transition metal complexes and development of these complexes as metallo-drugs.[17,18] Since there are many alterations in the genes that code for the protein in tumor, the focus of such studies is also on proteins which drive and control cell cycle progression.[19,20]

Herein, we describe the synthesis, characterization of D-glucose-bis pyrazolyl metal complexes of Cu(II) **1** and Ni(II) **2** and their binding properties with CT DNA. Furthermore, DNA cleavage of pBR322 DNA by complex **1** was carried out by employing agarose gel electrophoresis. The "binding study" of complex **1** towards human serum albumin (HSA), L-tryptophan and their mixtures with DNA was studied to recognize the most favoured biomolecule, for which it shows highest binding affinity.

Experimental

Materials and Methods D-Glucose, $CuCl_2\cdot2H_2O$, $NiCl_2\cdot6H_2O$ (Qualigens), pyrazole (Fluka). Tris (Tris=Tris(hydroxymethyl)aminomethane) base (Merck), 6× loading dye (Fermental Life Science) and super coiled plasmid DNA pBR322 (Genei) were utilized as received. Disodium salt of calf thymus DNA, human serum albumin and L-tryptophan were purchased from Sigma Chemical Company and stored at 4 °C. All reagent grade compounds were used without further purification.

Interspec 2020 FTIR spectrometer was used for recording IR spectra of KBr pellets in the range of 400—4000 cm^{-1}. Electronic spectra were recorded on UV-1700 PharmaSpec UV–vis spectrophotometer (Shimadzu). Data were reported in λ_{max}/nm. Emission spectra were determined with a Hitachi F-2500 fluorescence spectrophotometer. Microanalyses of the complexes were obtained on a Carlo Erba Analyzer Model 1108. ^{1}H- and ^{13}C-NMR spectra were recorded on a Bruker DRX-300 spectrometer. Chemical shifts were reported in δ scale. EPR spectrum of copper(II) complex was recorded on Varian E 112 spectrometer at the X-band frequency (9.1 GHz) at liquid nitrogen temperature (LNT) using tetracyanoethylene (TCNE) as field marker. Cyclic voltammetry was carried out at CH instrument electrochemical analyzer. All voltammetric experiments were performed in single compartmental cell of volume 10—15 ml containing a three-electrode system comprised of a Pt-disk working electrode, Pt-wire as auxiliary electrode and an Ag/AgCl electrode as reference electrode. The supporting electrolyte was 0.4 M KNO_3 in milli-Q water. Deaerated solutions were used by purging N_2 gas for 15 min prior to measurements. Molar conductance was measured at room temperature on Digisun electronic conductivity bridge. Interaction of complexes with calf thymus DNA was performed in 0.01 M Tris–HCl buffer (pH 7.2). Solutions of calf thymus DNA in buffer gave a ratio of absorbance at 260 nm and 280 nm of *ca.* 1.9 indicating that DNA was free from pro-

* To whom correspondence should be addressed. e-mail: tsartaj62@yahoo.com
© 2010 Pharmaceutical Society of Japan

tein.[21] Viscosity measurements were carried out using Ostwald's viscometer at 29±0.01 °C. Flow time was measured with a digital stopwatch. Each sample was measured three times and an average flow time was calculated. Data are presented as η/η_0 *versus* binding ratio [M]/[DNA].[22] Where η is a viscosity of DNA in the presence of complexes and η_0 is the viscosity of DNA alone. Viscosity values were calculated from the observed flow time of DNA containing solution ($t>100$ s) corrected for the flow time of buffer alone (t_0), $\eta=t-t_0$. The intrinsic binding constant, K_b and Stern–Volmer quenching constant, K of the complexes **1** and **2** to CT DNA were determined from Eq. 1 by UV–vis titrations and 2 (Stern–Volmer equations) by emission titrations, respectively.[23,24]

$$[DNA]/|\varepsilon_a-\varepsilon_f|=[DNA]/|\varepsilon_b-\varepsilon_f|+1/K_b|\varepsilon_b-\varepsilon_f| \quad (1)$$

$$I_0/I=1+Kr \quad (2)$$

Where [DNA] represents the concentration of DNA, ε_a, ε_f and ε_b are the apparent extinction coefficient A_{obs}/[M], the extinction coefficient for free metal [M] complex and the extinction coefficient for metal [M] complex in the fully bound form, respectively. In plots of $[DNA]/\varepsilon_a-\varepsilon_f$ *versus* [DNA], K_b is given by the ratio of slope to intercept. These absorption spectral titration experiments were performed in UV-1700 PharmaSpec UV–vis spectrophotometer (Shimadzu), by maintaining a constant concentration of metal complex while varying the nucleic acid concentration. This was achieved by dissolving an appropriate amount of metal complex and CT DNA stock solutions while maintaining the total volume constant (3 ml). A reference cell contained DNA alone to nullify the absorbance due to the DNA at the measured wavelength. The absorbance of broadened band in the intraligand regions of each investigated complex was recorded after successive addition of CT DNA. I_0 and I are fluorescence intensities in absence and presence of CT DNA, respectively. K is a linear Stern–Volmer quenching constant, r is the ratio of the total concentration of the complex to that of DNA, [M]/[DNA]. In the plot of I_0/I *vs.* r, the Stern–Volmer quenching constant K is given by the intercept. Emission intensity measurements were carried out using Hitachi F-2500 fluorescence spectrophotometer. Preliminary adjustments were carried out using Tris–HCl buffer as blank. The excitation wavelength was fixed and the emission range was adjusted before measurements. DNA was pretreated with ethidium bromide (EthBr) for 30 min at 25 °C. The metal complexes were then added to this mixture and their effect on the emission intensity was measured.

The cleavage of supercoiled pBR322 DNA in absence of activating agents was observed using gel electrophoresis. In reactions using supercoiled pBR322 DNA 300 ng in Tris–HCl (10 mmol) buffer at pH 7.4 were treated with complex **1** (0.05—0.2 mmol). The samples were incubated for 2 h at 37 °C. A loading buffer containing 25% bromophenol blue, 0.25% xylene cyanol, 30% glycerol was added and electrophoresis was carried out at 60 V for 2 h in Tris–HCl buffer using 1% agarose gel containing 1.0 μg/ml ethidium bromide. To identify the reactive oxygen species involved in cleavage reactions, the radical scavenger dimethyl sulfoxide (DMSO) (5%) was introduced.

The DNA cleavage with added reductant was monitored as in case of cleavage experiment without added reductant using agarose gel electrophoresis. Reactions using pBR322 DNA in Tris–HCl buffer at pH 7.4 was treated with complex **1** (0.025—0.1 mmol) and ascorbic acid (0.01 mmol). The samples were incubated for 0.5 h at 37 °C.

Similarly in photocleavage studies, reaction mixture was carried out under illuminated conditions at 365 nm (12 W) monochromatic light source. The samples were incubated for 1 h at 37 °C and analyzed for photocleaved products using gel electrophoresis as discussed above. Reaction using supercoiled pBR322 plasmid DNA in Tris–HCl was treated with complex **1** (0.05—0.2 mmol). All the gels were viewed by UVP gel doc system and photographed.

Synthesis. D-Glucose-bis pyrazolyl Cu(II) (1) To a solution of D-glucose (1.80 g, 10 mmol) in 10 ml H_2O was added $CuCl_2\cdot 2H_2O$ (1.71 g, 10 mmol) in 10 ml methanol; a green colored solution obtained was stirred for 2 h at room temperature. A solution of pryazole (1.36 g, 20 mmol) in 10 ml methanol was added slowly to the reaction mixture, a fluorescent green colored precipitate formed was filtered and washed thoroughly with methanol and dried *in vacuo*. Yield 44%. mp 180 °C. UV/VIS (H_2O): 747, 295, 220. IR (as KBr disc, cm^{-1}) 3318 ν (O–H), 2964 ν (C–H), 1637 δ (HOH), 1512 ν (C=C, C=N), 1324—1405 ν (C–C) ν (C–O), 1062—1101 ν(C–H), 553 ν (Cu–O), 429 ν (Cu–N). ESI-MS: 431 $[M]^+$. *Anal.* Calcd for $C_{12}H_{24}N_4O_9Cu$: C 33.37, H 5.60, N 12.97; Found: C 33.21, H 5.58, N 12.94.

D-Glucose-bis pyrazolyl Ni(II) (2) The complex **2** was synthesized with $NiCl_2\cdot 6H_2O$ (2.37 g, 10 mmol) by a similar method as described for **1**. The green colored product obtained was filtered, washed with methanol and dried *in vacuo*. Yield 38%. mp *ca.* 170 °C (decomp.). UV/VIS (H_2O): 644, 385, 220. IR (as KBr disc, cm^{-1}) 3346 ν (O–H), 2982 δ (C–H), 1635 δ (HOH), 1538 ν (C=C, C=N), 1324—1405 ν (C–C) ν (C–O), 1062—1101 ν (C–H), 590 ν (Ni–O), 430 ν (Ni–N). ^{1}H-NMR (400 MHz, D_2O, 25°, δ ppm): 3.2—4.8 (skeleton protons of D-glucose); 6.1—7.6 (arom. pyrazole H). ^{13}C-NMR (75.44 MHz, D_2O, 25°, δ ppm): 91, 75.9, 74.07, 72.6, 60.1 (skeletal carbon atoms of D-glucose from C_1—C_6); 95.79 (arom. C) ESI-MS: 499 $[M]^+$. *Anal.* Calcd for $C_{12}H_{32}N_4O_{13}Ni$: C 28.88, H 6.46, N 11.23; Found: C 28.84, H 6.44, N 11.21.

Results and Discussion

D-Glucose-bis pyrazolyl metal complexes **1** and **2** were synthesized by *in situ* reaction of metal complexes of D-glucose and pyrazole. These complexes were characterized by various analytical and spectroscopic methods. The coordination geometry around metal ion (M=Cu(II), Ni(II)) in **1** and **2** is square pyramidal. Spectroscopic studies and analytical data support proposed structure (Chart 1). All the complexes are soluble in H_2O, DMSO and DMF. The molar conductance measurements in H_2O show that **1** and **2** are non-ionic in nature. The binding studies with CT DNA were performed employing various techniques. Comparative *in vitro* binding study of complex **1** towards different biomolecules was also carried out to recognize the most favoured biomolecules which possess highest binding affinity.

IR Spectra The IR spectra of complexes **1** and **2** exhibit characteristic broad bands of metal bound saccharide moieties in comparison to corresponding simple metal ion adducts, which generally display sharp signals.[25] The broad and intense band observed in the range 3300—3416 cm^{-1} was assigned to ν (OH) and indicates the breakage of hydrogen bonding.[25] The secondary interaction of free hydroxyl groups with metal ions in these complexes was indicated by the shape, position and width of the bands. The ν (OH) of H_2O also appears in this region but was overlapped with the ν (OH) bands.[26] The IR spectra of **1** and **2** are shown in Fig. 1.

The bands observed at 2964 and 2982 cm^{-1} were assigned

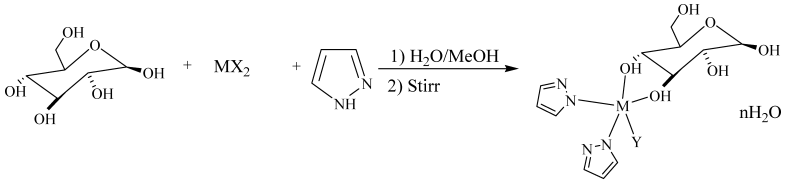

1 M= Cu,Y=H_2O, n = 2
2 M=Ni,Y=H_2O, n = 6
X=Cl

Chart 1. Proposed Structures of **1** and **2**

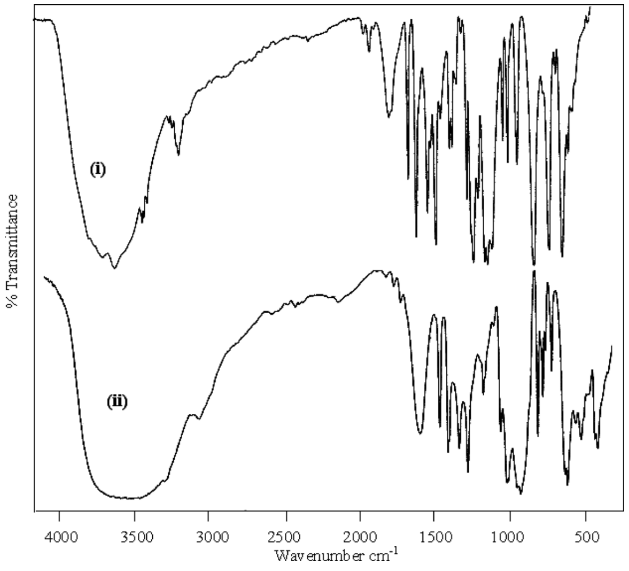

Fig. 1. IR Spectra of Complexes **1** (i) and **2** (ii)

to ν (CH) stretching vibrations.[27] The characteristic bands observed at 1637 cm^{-1}, 1635 cm^{-1} were attributed to δ (HOH), however, absorption bands at 1324—1405 cm^{-1} and 1062—1101 cm^{-1} were assigned to ν (C–C), ν (C–O) and ν (C–H), vibrations respectively.[4] Additionally, bands at *ca.* 1512 cm^{-1} and 1538 cm^{-1} observed in the IR spectra of **1** and **2** were attributed to ν (C=N–C=C) stretching vibration of pyrazole.[28—31] The far IR spectra of these complexes exhibit absorption bands at *ca.* 553, 590 cm^{-1} and 429, 430 cm^{-1} due to ν (M–O) and ν (M–N) vibrations, respectively (M=Cu, Ni) which reveal the binding of saccharide and secondary ligand to the metal ion.

NMR Spectra ^{1}H- and ^{13}C-NMR spectra of complex **2** were recorded in D_2O. Resonances arising from different saccharide protons generally overlap resulting in broadening of signals, and thereby individual resonances are difficult to identify. However, complex **2** revealed broad envelope with fine structure at δ 3.1—4.8 ppm attributed to strongly coupled skeletal proton signals of saccharides.[32] The signals at *ca.* 6.1—7.6 ppm were attributed to the aromatic protons of pyrazole ring, respectively.[28] However, resonances due NH of heterocyclic moiety were not observed in both the complexes, indicating, the formation of complex occurs through dissociation of NH protons. Based on the coordination induced shifts $\Delta\delta$ (CIS=$\delta_{complex}-\delta_{ligand}$), **2** exhibited maximum shifts with C-3 and C-4 carbon atoms $\Delta\delta$=1.7 and 1.2 respectively, indicating the favorable interaction of C-3 and C-4 hydroxyls with the metal ions though other carbon signals shifted to different extents due to the influence of metal ion binding.[33] The $\Delta\delta$ values indicate that the metal ions bound to saccharide OH of C-3 and C-4 atoms, in comparison to saccharide O^-, which gives higher $\Delta\delta$ values.[26] The complex **2** also revealed ^{13}C resonances at 95.79 and 126 ppm, respectively which were assigned to carbon skelton of pyrazole ligand.[25]

EPR Spectrum The X-band EPR spectrum of **1** was recorded at liquid nitrogen temperature (LNT) in solid state using tetracyanoethylene (g=2.00277) as field marker. The EPR spectrum of **1** exhibited a broad band having 'g' isotropic values 2.09 which are characteristic for square pyramidal enviroment. Similar spectra having 'g' isotropic values were reported earlier[34,35] for metal saccharide complexes composed of different metal ions. Such isotropic lines usually result due to intermolecular spin exchange, which broadens the spectral lines. This intermolecular spin exchange is caused by the strong spin coupling, which occurs during collision of paramagnetic centers.

UV–Vis Spectra The electronic spectra measurement of freshly prepared aqueous solutions of **1** and **2** were carried out in the region 200—1100 nm. The UV–vis spectra of **1** revealed prominent bands at 747 nm attributed to $d_{xz}, d_{yz} \rightarrow d_{x^2-y^2}$ ligand field transitions,[36,37] which are followed by a shoulder and strong bands in the UV region at 295, 246 and 220 nm assigned to the ligand to metal charge transfer (LMCT) and intraligand charge transfer (IL) bands, respectively. These results are typical of square pyramidal geometry around Cu^{2+} metal ion.[36,37] The bands at 747 nm thus confirm the square pyramidal geometry of **1** as deduced by EPR studies.

The electronic spectrum of complex **2** displayed a similar spin allowed transition at 644 assigned to $^3B_1(F) \rightarrow {}^3E(F)$ transitions. These values are consistent with pentacoordinate geometry around Ni^{2+} metal ion.[38,39] The spectra also exhibited LMCT transition at 385 and 300 nm in addition to IL band at 220 nm, respectively.

DNA Binding Studies. UV–Vis Absorption Titration The interaction of complexes **1** and **2** with CT DNA was carried out by titrating fixed amount of complexes (0.067×10^{-4} M) with increasing concentration of CT DNA (R=0—4.97, R=[DNA]/[**1**, **2**]). The absorption spectra of complexes reveal hyperchromism with no blue or red shift at 260 nm, however, slight red shift (1—2 nm) at 210 nm was observed in the intraligand (IL) charge transfer bands. A similar hyperchromic effect has been observed for IL bands of certain metal complexes when interacted with CT DNA.[40] The percentage hyperchromism observed was found to be independent of the concentration of added DNA, revealing that the origin of hyperchromism might lie in the mechanism of interaction of the complex with DNA. The percent hyperchromism observed for **1** and **2** is given in Table 1. Further the "hyperchromic effect" observed on the addition of CT DNA to **1** and **2** reflects the structural damage to the secondary structure of DNA duplex as a consequence of strong binding of the complexes.[41] This is attributed to the covalent binding of the complexes to the CT DNA *via* N7 of guanine nucleobase of DNA double helix. Furthermore, the presence of heterocyclic rings can facilitate partial intercalation by insertion of the complexes into the adjacent base pairs of DNA. The binding strength of **1** and **2** has been compared quantitatively by calculating K_b values using Eq. 1, monitoring the changes in IL bands with increasing concentration of CT DNA (Figs. 2i, ii). The K_b values of **1** and **2** are shown in Table 1. The K_b value of **1** shows multifold increase in comparison to K_b value of **2**, which has been attributed to the stronger affinity of copper complexes for sequence specific binding to N7 nucleobase of DNA.[42] Copper complexes are avid DNA binders in comparison to other transition metal complexes.[42] The K_b values of the complexes are smaller than classical intercalators ethidium bromide (where K_b values are in the order of $10^7\ M^{-1}$),[43] therefore intercalating mode of binding of complexes to DNA is ruled out.

Comparative Binding Studies In a drug delivery, cellu-

Table 1. Absorption Spectral and Emission Properties of Complexes **1** and **2** Bound to CT DNA

Complex	K_b (10^5 M^{-1})	*Kr*	% Hyperchromism
1	13.4	1.33	54
2	4.5	0.55	50

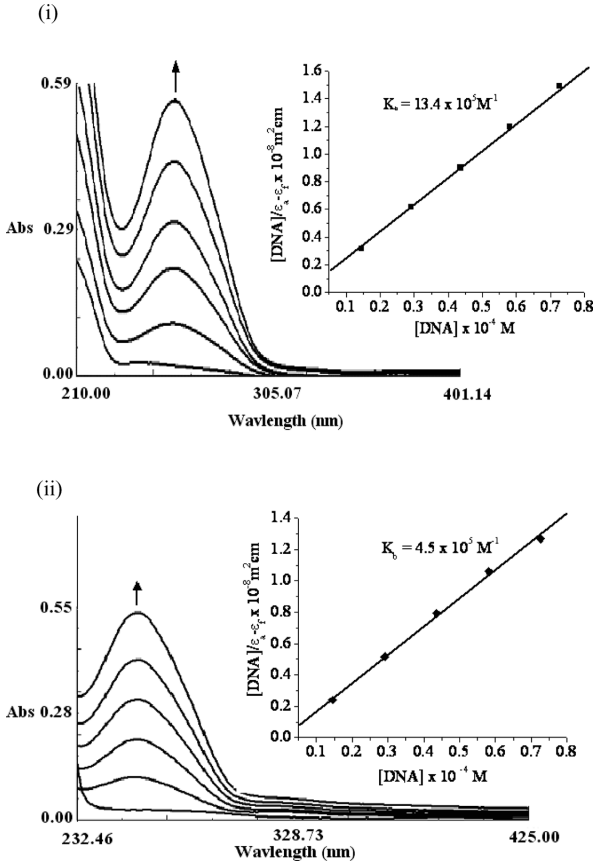

Fig. 2. Absorption Spectral Traces of **1** (i) and **2** (ii) in Tris–HCl Buffer upon Addition of CT DNA

Inset; plots of [DNA]/$\varepsilon_a-\varepsilon_f$ *versus* [DNA] for the titration of CT DNA with complexes, (■), (◆) experimental data points; full lines, linear fitting data.

lar uptake processes aquation and interaction of drugs with biologically relevant molecules like serum transport proteins and DNA plays important role in its mode of action.[44,45] Tryptophan plays a fundamental role in membrane proteins. The indole side chain has both hydrophobic and hydrophilic character, and consequently, it partitions at the hydrophobic–hydrophilic interface in lipid bilayers.[46] Tryptophan may indeed play an important role in stabilizing membrane proteins through electrostatic interactions at the lipid bilayer surface. Recently, it has been suggested through computational,[47] electrophysiological,[48] fluorescence[49] and NMR[50] studies that the indole N–H groups may have hydrogen bonding with the aqueous interface or directly to the lipid molecules. This appears to stabilize the protein in the bilayer.[48] Furthermore, the indole possesses a substantial permanent dipole moment. The orientation of this dipole moment may have a significant effect on the ionic interactions of membrane proteins, and in this molecular system the tryptophan dipole moment appears to have a direct effect on the conductance of cations. Therefore, based on these reasons we can conclude that metal complexes before encountering the DNA has to pass through the membrane consisting of proteins rich in aminoacids and how much binding affinity is exhibited by metal complexes towards these aminoacids, particularly tryptophan. Indole, an electron-rich aromatic moiety is known to form a hydrophobic environment in proteins and to be involved in enzymatic reactions. In addition to the redox activities and various weak interactions, it shows versatile metal binding abilities through the nitrogen and carbon atoms. The review focusing on the properties of the indole ring in and around the coordination sphere and the structures and bonding modes of Cu(I), Cu(II), Pd(II), and Pt(II) complexes of indole-containing ligands has been recently published by Shimazaki *et al.*[51] in which they have discussed the structures, and reactivities of the indole ring as observed for the metal complexes with various ligands including 3N-, 2N1O-, and 2N-tripod-like ligands containing one or two proximal indole rings. Therefore from these observations it is probable that L-tryptophan can interact with the metal complex *via* coordination through indole N-atom to occupy the vacant sixth coordination site.

The comparative binding studies have been monitored by different methods,[52—55] which have emerged as important tool in metallo-drug discovery. We have utilized absorption spectral method to carry out an *in vitro* "binding study" of complex **1** with biomolecules (HSA, L-tryptophan) and their mixtures with CT DNA. The absorption spectral titration, at a constant concentration of **1** (0.067×10^{-4} M) was carried out with increasing concentration of biomolecules (DNA, HSA, L-tryptophan) (R=0—4.97, R=[biomolecules]/[**1**], and their mixtures). The spectral titration of **1** with HSA exhibit a hyperchromism with a red shift at 201, 277 nm of 14 nm and 3 nm, respectively, however no shift was observed at 260 nm. On increasing the concentration of L-tryptophan, the absorption spectra of **1** displayed hyperchromic effect with no batho or hypsochromic shift at 218 nm and 260 nm. The intrinsic binding constant K_b were 3.16×10^5 M^{-1} and 4.33×10^5 M^{-1} for HSA and L-tryptophan, respectively.

The mixtures of HSA and CT DNA exhibited hyperchromism at 200 nm and 260—277 nm. A bathochromic shift of 14 nm was observed at 260—277 nm. On increasing the equimolar ratio of HSA and DNA mixture, a sharp decrease in binding constant value (3.5×10^4 M^{-1}) in comparison to that for DNA alone was observed. The absorption spectral titration of mixtures of L-tryptophan and CT DNA revealed hyperchromism at 218, 260—280 nm with no red shift. The K_b value (7.14×10^5 M^{-1}) was almost half in magnitude in comparison to that for CT DNA. Similarly, the absorption titration of mixtures of HSA, L-tryptophan and DNA also featured hyperchromism at 200 and 260—280 nm with a red shift of 14 nm at 200 nm wavelength. The K_b value was more than 100 times lower in magnitude in comparison to that of CT DNA. The K_b values of complex **1** towards these biomolecules and their mixtures are shown in Table 2. Therefore, comparative binding study of **1** with human serum albumin, L-tryptophan and their mixtures with CT DNA were carried out to recognize the most favored biomolecule for which it displays highest binding ability, further multifold decrease in binding ability of **1** with mixtures of these biomolecules were observed. On the basis of absorption spectral data, it was observed that **1** shows highest affinity towards the main cellular

target DNA.

Cyclic Voltammetry Cyclic voltammetry has been used to probe the interaction (electrostatic or intercalation) of metal complexes with CT DNA.[56] This technique has been successfully employed to discriminate the enantioselective interaction of metal complexes with CT DNA.[57] The application of cyclic voltammetry to the study of interaction of redox-active metal complexes with DNA provides a useful complement to the spectral and viscometeric studies. The cyclic voltammetric (CV) responses of **1** and **2** in the absence and presence of CT DNA are well defined (Figs. 3i, ii). The cyclic voltammograms of **1** and **2** in the absence of DNA reveal a non-Nerstian but fairly reversible/quasireversible one electron redox process involving M^n/M^{n-1} couple (M=Cu, Ni, $n=2$) as judged from peak potential separation of 0.081—0.386 V (0.59 V for a one electron transfer process). For both complexes, the peak current ratios I_{pa}/I_{pc} are far from unity (unity for chemically reversible redox system), suggesting a quasireversible electron transfer. At different scan rates (0.1—0.3 $V\,s^{-1}$), the cyclic volatmmograms of **1** and **2** do not show any major changes. On addition of CT DNA to the complexes, the peak potential separation ΔE_p decreases. The $E_{1/2}$ values of DNA-bound complexes follow the same order as that for free complexes. The net shift in $E_{1/2}$ can be used to estimate the ratio of equilibrium constants for M^{n+} and $M^{(n-1)+}$ complexes to DNA using equation,

$$E_b^{o\prime} - E_f^{o\prime} = 0.059 \log(K^+_{(n-1)}/K^+_n)$$

Where $E_b^{o\prime}$, $E_f^{o\prime}$ are the formal potentials of $M^{n+}/M^{(n-1)+}$ couples in the free and bound forms, respectively and K_{n-1}, K_n are corresponding binding constants for the binding of $(n-1)$ and n species to DNA, respectively. The $K^+_{(n-1)}/K^+_n$ are binding constants for respective species to DNA. Interestingly $K^+_{(n-1)}$ and K^+_n values of complexes **1** and **2** are near unity, which suggest that they are involved in DNA interaction favoring both oxidation states equally. A similar observation has been made by Mahadaven *et al.*[58—60] Furthermore, the significant shift in the electrode potentials and peak current ratios on addition of CT DNA can be explained in terms of the diffusion of an equilibrium mixture of free and DNA bound metal complexes to the electrode surface[61] thus implying a strong binding of **1** and **2** with CT DNA. A summary of the voltammetric results for the complexes **1** and **2** in the absence and the presence of CT DNA are given in Table 3.

Fluorescence Spectral Studies The interaction between complexes **1** and **2** with CT DNA was also investigated by changes in fluorescence characteristics of the complexes upon binding to the CT DNA. Competitive ethidium bromide (EthBr) binding study was undertaken to understand the mode of CT DNA interaction of **1** and **2**. The molecular fluorophore EthBr emits intense fluorescence in the presence of CT DNA due to its strong intercalation between the adjacent DNA base pairs. The addition of the second molecule, which binds to DNA more strongly than EthBr, would quench the DNA-induced EthBr.[62] The extent of quenching of the fluorescence of EthBr bound to DNA would reflect the extent of DNA binding of the second molecule. On addition of com-

Table 2. Absorption Spectral Properties of Complex **1** Bound to CT DNA, HSA, L-Tryptophan, HSA+DNA, L-Tryptophan+DNA, HSA+L-Tryptophan+DNA

Complex **1**	K_b
DNA	13.4 ($10^5\,M^{-1}$)
HSA	3.16 ($10^5\,M^{-1}$)
Tryptophan	4.33 ($10^5\,M^{-1}$)
HSA+DNA	3.5 ($10^4\,M^{-1}$)
Tryptophan+DNA	7.14 ($10^4\,M^{-1}$)
HSA+tryptophan+DNA	1.16 ($10^4\,M^{-1}$)

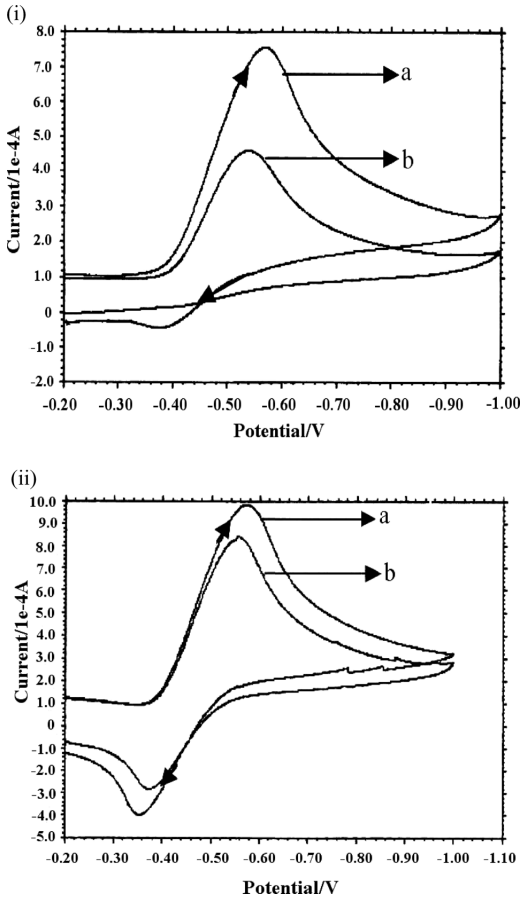

Fig. 3. Cyclic Voltammograms of **1** (i) and **2** (ii) at a Scan Rate 0.3 $V\,s^{-1}$ in H_2O (a) **1** and **2** in the Absence of CT DNA, (b) **1** and **2** in the Presence of CT DNA

Table 3. Cyclic Voltammetric Results of Complexes **1** and **2** in the Absence and Presence of CT DNA

Complex	E_{pc} (V)	E_{pa} (V)	$E_{1/2}$ (V)	ΔE_p (V)	I_{pa}/I_{pc}	$K^+_{(n-1)}/K^+_n$
1	−0.5651	−0.3718	−0.468	0.386	0.5446	1.37
1+DNA	−0.539	−0.3804	−0.46	0.1595	0.25	
2	−0.5707	−0.3533	−0.462	0.217	0.382	1.08
2+DNA	−0.552	−0.3725	−0.46	0.179	0.3322	

plexes (6.67×10^{-5}—33×10^{-5} M) to DNA pretreated with EthBr ([DNA]/[EthBr]=1) the decrease in emission intensity was observed (Figs. 4i, ii). The emission intensity in absence and presence of CT DNA of **1** and **2** is depicted in Fig. 5. Two mechanisms have been proposed to account for quenching of EthBr emission, the replacement of molecular fluorophore and/or electron transfer. The non replacement-based quenching has been suggested with DNA-mediated electron transfer from the excited ethidium bromide to acceptor **1** and **2** metal complexes. If all the complexes follow any one of the two mechanisms then the extent of replacement of EthBr should be higher than the observed values. As there is no complete quenching of the EthBr-induced emission intensity, an intercalative mode of DNA-binding of **1** and **2** observed values is ruled out. Further, the quenching extents "*K*" for **1** and **2** have been estimated by using Stern–Volmer Eq. 2 and are given in Table 1. The enhanced "*K*" values for complexes **1** supports absorption spectral studies. A possible mode of binding could be covalent binding of **1** and **2** with the nitrogen donors of purine, which might facilitate the uncoiling of double strand, thus decreasing the DNA-EthBr fluorescence intensity.[63]

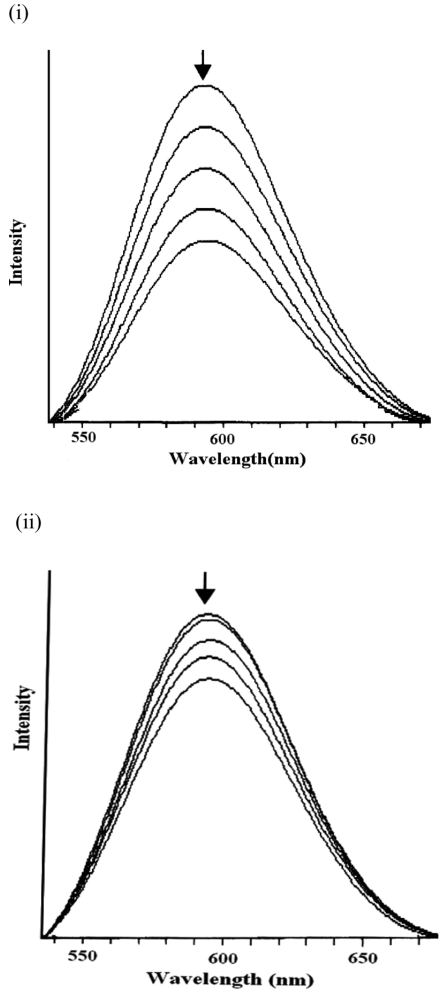

Fig. 4. Emission Spectra of **1** (i) and **2** (ii) in the Presence of DNA in Tris–HCl Buffer

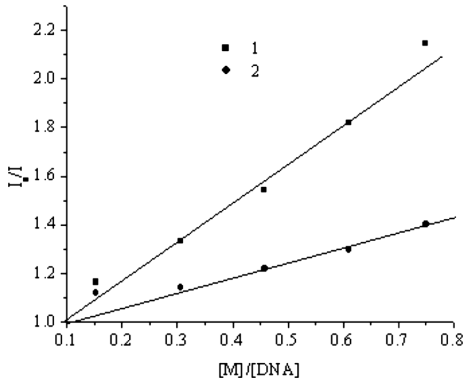

Fig. 5. Plots of I_0/I *versus* [M]/[DNA], [M]=[**1**], [**2**]

DNA Cleavage Studies The potential of metal complexes to act as nuclease mimic agents and enhance the cleavage of nucleic acids has attracted significant attention.[64—66] The role of metal complexes in DNA hydrolysis appears to include the positioning of both the substrate and of a coordinated water to act as an activated nucleophile.[67] The DNA cleavage ability of the complex **1** was assessed by incubating it with supercoiled (SC) pBR322 DNA in Tris–HCl buffer for 2 h without addition of a reductant. The reaction mixture was subjected to agarose gel electrophoresis and a concentration dependant DNA cleavage was observed Fig. 6i. With increase in concentration of **1** more intense nicked form (Form II) was observed, whereas there was no conversion to linear form (Form III). Form I and II of pBR322 DNA were visible on the gel indicating that **1** was involved in DNA cleavage.

To ascertain whether any favorable reducing agent added to the reaction mixture could account for increased supercoiled pBR322 DNA degradation by **1**, cleavage reaction was performed in aerobic conditions by adding ascorbic acid to the reaction mixture containing supercoiled pBR322 DNA in Tris–HCl buffer (Fig. 6ii). In the control experiment using ascorbic acid alone, no cleavage of pBR322 DNA was observed. On increasing the concentration of **1** complete conversion of SC (Form I) to NC (Form II) and LC (Form III) was observed involving a double strand DNA cleavage.[68] The increased nuclease activity of **1** is apparently caused by enhanced stabilization of Cu(I) species formed by reduction of **1** by ascorbic acid. This suggests a probable mechanism involving the generation of hydroxyl radicals from ascorbic acid.[69] Similar hydroxyl radical promoted DNA damages have been reported.[70] Furthermore, when the hydroxyl radical scavenger DMSO was added to the reaction mixture of **1**, the cleavage reaction was inhibited, revealing that a freely diffusible hydroxyl radical is the reactive oxygen species directly responsible for initiation of cleavage reaction.

The DNA cleavage activity of **1** with increasing concentration were also carried out using SC pBR322 DNA in Tris–HCl buffer and upon irradiation with UV light of 365 nm (Fig. 6iii) and involves double strand DNA cleavage to generate nicked form through single-strand breaks,[70] revealing that **1** is an active species. Addition of hydroxyl radical scavenger DMSO to the reaction mixture tends to inhibit the cleavage reaction, suggesting the involvement of hydroxyl radical, in the photocleavage reactions. It can be suggested that photoexcited complex would follow a mechanistic pathway involving one or two electron reduction of the oxygen molecule to generate hydroxyl radicals rather than conversion of oxygen molecule to singlet oxygen, which is gener-

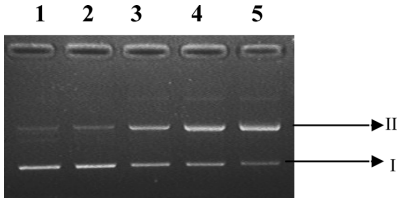

Fig. 6i. Gel Electrophoresis Diagram Showing Cleavage of pBR322 Supercoiled DNA (300 ng) by **1**; Lane 1: DNA; Lane 2: 0.05 mmol **1**+DNA; Lane 3: 0.10 mmol **1**+DNA; Lane 4: 0.15 mmol **1**+DNA; Lane 5: 0.20 mmol **1**+DNA

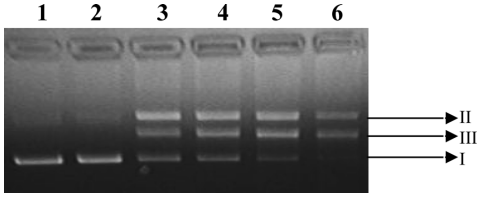

Fig. 6ii. Gel Electrophoresis Diagram Showing Cleavage of pBR322 Supercoiled DNA (300 ng) by **1** in Presence of Radical Scavenger (5% DMSO) and Ascorbic Acid H_2A (0.01 mmol); Lane 1: DNA+**1**+DMSO; Lane 2: DNA; Lane 3: 0.025 mmol **1**+H_2A+DNA; Lane 4: 0.05 mmol **1**+H_2A+DNA; Lane 5: 0.075 mmol **1**+H_2A+DNA; Lane 6: 0.10 mmol **1**+H_2A+DNA+5% DMSO

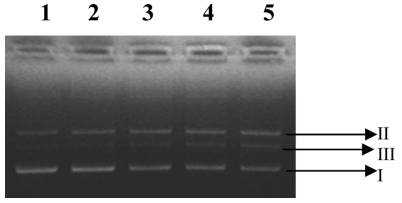

Fig. 6iii. Gel Electrophoresis Diagram Showing Cleavage of pBR322 Supercoiled DNA (300 ng) by **1** Using Monochromatic Radiation (365 nm) for 5 min Followed by Incubation (1 h); Lane 1: DNA; Lane 2: 0.05 mmol **1**+DNA; Lane 3: 0.10 mmol **1**+DNA; Lane 4: 0.15 mmol **1**+DNA; Lane 5: 0.20 mmol **1**+DNA

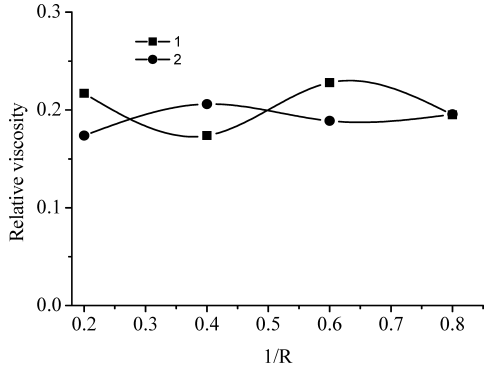

Fig. 7. Effect of Increasing Amount of **1** and **2** on Relative Viscosity of CT-DNA at 29±0.1 °C

[DNA]=1×10^{-3} M, $1/R$=[M]/[DNA], [M]=[**1**, **2**].

ally observed in the photodynamic therapy cycle.[71]

Viscosity Measurements To further explore the binding mode of complexes **1** and **2** to CT DNA, viscometric studies were carried out by measuring the flow rate of CT DNA through a viscometer as a function of concentration of added complexes ($1/R$=[M]/[DNA], (M=**1**, **2**). The hydrodynamic changes are result of the changes in length of molecules, the diminished bending between layers and the diminished length-specific mass.[72] The decrease in relative viscosity observed for **1** and **2** suggest the hydrophobic interaction between complexes with DNA surface, encouraged by partial intercalation and covalent bonding interaction, leading to bending (kinking) of the DNA chain.[73,74] The relative specific viscosity of DNA with increasing the concentration of **1** and **2** is shown in Fig. 7.

Conclusion

New metal complexes **1** and **2** have been isolated and characterized by various spectroscopic techniques with an aim to develop robust cancer chemotherapeutic agents. Complexes **1** and **2** possess a square pyramidal geometry as diagnosed by ligand field and EPR spectra. The DNA binding studies reveal a covalent binding mode of **1** and **2** and to CT DNA. *In vitro* model binding study of complex **1** with different biomolecules and their mixtures with CT DNA also support that the DNA is the most favored biomolecule. Complexes **1** and **2** also facilitate the quenching of ethidium bromide induced DNA emission by stabilizing the DNA conformation. Plasmid circular DNA (pBR322) cleavage experiments of complex **1** have been carried out employing gel electrophoresis. The complex **1** shows a unique ability to affect DNA double strand scission by hydrolytic (in absence of a reductant), oxidative and photocleavage reactions. Therefore, it is proposed that newly synthesized D-glucose-bis pyrazolyl Cu(II) complex **1** can be a better DNA binding and cleaving agent.

Acknowledgements We are grateful to the University Grants Commission, New Delhi for financial support through Research Grant No. 31-100/2005 and Third World Academy of Science, Italy (Grant No. 01-268RG/CHE/AS) for generous financial support to purchase electrochemical analyzer. Thanks to Regional Sophisticated Instrumentation Center, Central Drug Research Institute, Lucknow, for providing CHN-analysis data, ESI-Mass and NMR spectra and Regional Sophisticated Instrumentation Center, Indian Institute of Technology, Bombay, for EPR measurements.

References

1) Storr T., Thompson K. H., Orvig C., *Chem. Soc. Rev.*, **35**, 534—544 (2006).
2) Gyurcsik B., Nagy L., *Coord. Chem. Rev.*, **203**, 81—149 (2000).
3) Rao C. P., Das T. M., *Indian J. Chem.*, **42A**, 227—239 (2003).
4) Sreedhara A., Rao C. P., Rao B. J., *Carbohydr. Res.*, **289**, 39—53 (1996).
5) Bertazzi N., Bruschetta G., Casella G., Pellerito L., Rotondo E., Scopelliti M., *Appl. Organometal. Chem.*, **17**, 932—939 (2003).
6) Chen Y., Heeg, M. J., Braunschweiger P. G., Xie W., Wang P. G., *Angew. Chem. Int. Ed.*, **38**, 1768—1769 (1999).
7) MacLean G. D., Miles D. W., Rubens R. D., Reddish M. A., Longenecker B. M., *Emphasis Tumor Immunol.*, **19**, 309—316 (1996).
8) Slovin S. F., Ragupathi G., Adluri S., Ungers G., Terry K., Kim S., Spassova M., Bornmann W. G., Fazzari M., Dantis L., Olkiewicz K., Lloyd K. O., Livingston P. O., Danishefsky S. J., Scher H. I., *Proc. Natl. Acad. Sci. U.S.A.*, **96**, 5710—5715 (1999).
9) Nakase I., Lai H., Singh N. P., Sasaki T., *Int. J. Pharm.*, **354**, 28—33 (2008).
10) Zhang Y., Yang R., Feng L., Li K., *Anal. Chem.*, **76**, 7336—7345 (2004).
11) Kufelnicki A., Wozniczka M., Checinska L., Miernicka M., Budzisz E., *Polyhedron*, **26**, 2589—2596 (2007).
12) Evans I. R., Howard J. A. K., Howard L. E. M., Evans J. S. O., Jacimovic Z. K., Jevtovic V. S., Leovac V. M., *Inorg. Chim. Acta*, **357**, 4528—4536 (2004).
13) Bandwar R. P., Rao C. P., *J. Inorg. Biochem.*, **68**, 1—6 (1997).
14) Hecht S. M., *Acc. Chem. Res.*, **19**, 383—392 (1986).
15) Goldberg I. H., *Acc. Chem. Res.*, **24**, 191—198 (1991).
16) Dedon P. C., Salzberg A. A., Xu J., *Biochemistry*, **32**, 3617—3622

(1993).
17) Chikira M., Tomizava Y., Fukita D., Sugizaki T., Sugawara N., Yamazaki T., Sasano A., Shindo S., Palaniandavar M., Anthroline W. E., *J. Inorg. Biochem.*, **89**, 163—173 (2002).
18) Oliver M. B., Garcia-Raso A. T., Molins A. E., Preito M. J., Moreno V., Martinez J., Llado V., Lopez I., Gutierrez A., Escriba P. V., *J. Inorg. Biochem.*, **101**, 649—659 (2007).
19) Sielecki T. M., Boylan J. F., Benfield P. A., Trainor G. L., *J. Med. Chem.*, **43**, 1—18 (2000).
20) Zang Z., Jin L., Qian X., Wei M., Wang Y., Wang J., Yang Y., Xu Q., Xu Y., Liu F., *ChemBioChem*, **8**, 113—121 (2007).
21) Marmur J., *J. Mol. Biol.*, **3**, 208—218 (1961).
22) Cohen G., Eisenberg H., *Biopolymers*, **8**, 45—55 (1969).
23) Lakowicz J. R., Webber G., *Biochemistry*, **12**, 4161—4170 (1973).
24) Liu G. D., Liao J. P., Huang S. S., Shen G. L., Yu R. Q., *Anal. Sci.*, **17**, 1031—1036 (2001).
25) Mukhopadhyay A., Kolehmainen E., Rao C. P., *Carbohydr. Res.*, **324**, 30—37 (2000).
26) Kaiwar S. P., Bandwar R. P., Raghavan M. S. S., Rao C. P., *Carbohydr. Res.*, **106**, 743—752 (1994).
27) Das T. M., Rao C. P., Kolehmainen E., Kadam R. M., Sastry M. D., *Carbohydr. Res.*, **337**, 289—296 (2002).
28) Effendy, Lobbia G. G., Pettinari C., Santini C., Skelton B. W., White A. H., *Inorg. Chim. Acta*, **308**, 65—72 (2000).
29) Das S., Pal S., *J. Mol. Struc.*, **753**, 68—79 (2005).
30) Lane T. J., Nakagawa C. S. C. I., Walter J. L., Kandathil C. S. C. A. J., *Inorg. Chem.*, **1**, 267—276 (1962).
31) Pettinari C., Pettinari R., Pellei M., Lobbia G. G., *Polyhedron*, **18**, 1941—1951 (1999).
32) Mukhopadhyay A., Karkamkar A., Kolehmainen E., Rao C. P., *Carbohydr. Res.*, **311**, 147—154 (1998).
33) Tabassum S., Mathur S., *J. Carbohydr. Chem.*, **24**, 865—887 (2005).
34) Youngme S., Phatchimkun J., Wannarit N., Chaichit N., Meejoo S., Albada G. A. V., Reedijk J., *Polyhedron*, **27**, 304—318 (2008).
35) Youngme S., Phuengphai P., Chaichit N., Albada G. A. V., Tanase S., Reedijk J., *Inorg. Chim. Acta*, **358**, 3267—3271 (2005).
36) Matsumoto K., Sekine N., Arimura K., Ohaba M., Sakiyama H., Okawa H., *Bull. Chem. Soc. Jpn.*, **77**, 1343—1352 (2004).
37) Balamurugan R., Palaniandavar M., Halcrow M. A., *Polyhedron*, **25**, 1077—1088 (2006).
38) Santana M. D., Garcia G., Rufete A., Arellano M. C. R., Lopez G., *J. Chem. Dalton Trans.*, **2000**, 619—625 (2000).
39) Santana M.D., Garcıa G., Navarro C. M., Lozano A. A., Perez J., Garcıa L., Lopez G., *Polyhedron*, **21**, 1935—1942 (2002).
40) Chen J., Wang X., Shao Y., Zhu J., Li Y., Xu Q., Guo Z., *Inorg. Chem.*, **46**, 3306—3312 (2007).
41) Arjmand F., Chauhan M., *Helv. Chim. Acta*, **88**, 2413—2423 (2005).
42) Sorokin V. A., Valeev V. A., Gladchenko G. O., Sysa I. V., Blagoi Y. P., Volchock I. V., *J. Inorg. Biochem.*, **63**, 79—98 (1996).
43) Cory M., Mckee D. D., Kagan J., Hanry D. W., Miller J. A., *J. Am. Chem. Soc.*, **107**, 2528—2536 (1985).
44) Pluim D., van Waardenburg R. C., Beijnen J. H., Schellens J. H., *Cancer Chemother. Pharmacol.*, **54**, 71—78 (2004).
45) Brabec V., Novakova O., *Drug Resist. Updates*, **9**, 111—112 (2006).
46) Jacobs R. E., White S. H., *Biochemistry*, **28**, 3421—3437 (1989).
47) Meulendijks G. H. W. M., Sonderkamp T., Dubois J. E., Nielsen R. J., Kremers J. A., Buck H. M., *Biochim. Biophys. Acta*, **979**, 321—330 (1989).
48) O'Connell A. M., Koeppe R. E. II, Andersen, O. S., *Science*, **250**, 1256—1259 (1990).
49) Scarlatta S. F., *Biochemistry*, **30**, 9853—9859 (1991).
50) Lazo N. D., Hu W., Cross T. A., *J. Chem. Soc., Chem. Commun.*, 1529—1531 (1992).
51) Shimazaki Y., Yajima T., Takani M., Yamauchi O., *Coord. Chem. Rev.*, **253**, 479—492 (2009).
52) Hartinger C. G., Timerbaev A. R., Keppler B. K., *Electrophoresis*, **24**, 2023—2037 (2003).
53) Timerbaev A. R., Hartinger C. G., Keppler B. K., *Trends Anal. Chem.*, **25**, 868—875 (2006).
54) Timerbaev A. R., Hartinger C. G., Aleksenko S. S., Keppler B. K., *Chem. Rev.*, **106**, 2224—2248 (2006).
55) Casini A., Gabbiani C., Mastrobuoni G., Messori L., Moneti G., Pieraccini G., *ChemMedChem*, **1**, 413—417 (2006).
56) Carter M. T., Rodriguez M., Bard A. J., *J. Am. Chem. Soc.*, **111**, 8901—8911 (1989).
57) Mahadevan S., Palniandavar M., *Bioconjg. Chem.*, **7**, 138—143 (1996).
58) Mahadevan S., Palniandavar M., *Inorg. Chem.*, **37**, 3927—3934 (1998).
59) Mahadevan S., Palniandavar M., *Inorg. Chem.*, **37**, 693—700 (1998).
60) Mahadevan S., Palniandavar M., *Inorg. Chim. Acta*, **254**, 291—302 (1997).
61) Hirohama T., Kuranuki Ebina Y., Sugizaki E. T., Arii H., Chikira M., Selvi P. T., Palaniandavar M., *J. Inorg. Biochem.*, **99**, 1205—1219 (2005).
62) Liu C., Zhou J., Xu H., *J. Inorg. Biochem.*, **71**, 1—6 (1198).
63) Rupesh K. R., Deepalatha S., Krihnaveni M., Venkatesan R., Jayachandran S., *Eur. J. Med. Chem.*, **41**, 1494—1503 (2000).
64) Itoh T., Hisada H., Sumiya T., Hosona M., Usui Y., Fuji Y., *Chem. Commun.*, **19**, 677—678 (1997).
65) Trewick B. N., Daniheer A. T., Bashkin J. K., *Chem. Rev.*, **98**, 939—960 (1998).
66) Cowan J. A., *Curr. Opin. Chem. Biol.*, **5**, 634—642 (2001).
67) Geyer C. R., Sen D., *Chem. Biol.*, **4**, 579—593 (1997).
68) Melvin M. S., Tomlinson J. T., Saluta G. R., Kucera G. L., Lindquist N., Manderville R. A., *J. Am. Chem. Soc.*, **122**, 6333—6334 (2000).
69) Ramakrishnan S., Rajendiran V., Palanaindavar M., Periasamy V. S., Srinag B. S., Krishnamurthy H., Akbarsha M. A., *Inorg. Chem.*, **48**, 1309—1322 (2009).
70) Santra B. K., Reddy P. A. N., Neelakanta G., Mahadevan S., Nethaji M., Chakravarty A. K., *J. Inorg. Biochem.*, **89**, 191—196 (2002).
71) Collet M., Hoebeke M., Piette J., Jakobs A., Lindqvist L., Vorst A. V., *J. Photochem. Photobiol. B*, **35**, 221—231 (1996).
72) Lerman L. S., *J. Mol. Biol.*, **3**, 18—30 (1961).
73) Raja A., Rajendran V., Maheswari P. U., Balamurugan R., Kilner C. A., Halcrow M. A., Palaniandavar M., *J. Inorg. Biochem.*, **99**, 1717—1732 (2005).
74) Liu J., Zhang H., Chen C., Deng H., Lu T., Ji L., *Dalton Trans.*, **2003**, 114—119 (2003).